

Supporting Information

**Crystal Design of Polar One-Dimensional
Hydrogen-Bonded Copper Coordination Complexes**

Kiyonori Takahashi, Norihisa Hoshino, Takashi Takeda, Koichiro Satomi, Yasutaka Suzuki,
Shin-ichiro Noro, Takayoshi Nakamura, Jun Kawamata, Tomoyuki Akutagawa

Infrared Spectroscopy.

Infrared (IR) absorption spectra under ambient condition were measured as KBr disks on Thermo Fisher Scientific's Nicolet 6700 FT-IR Smart System.

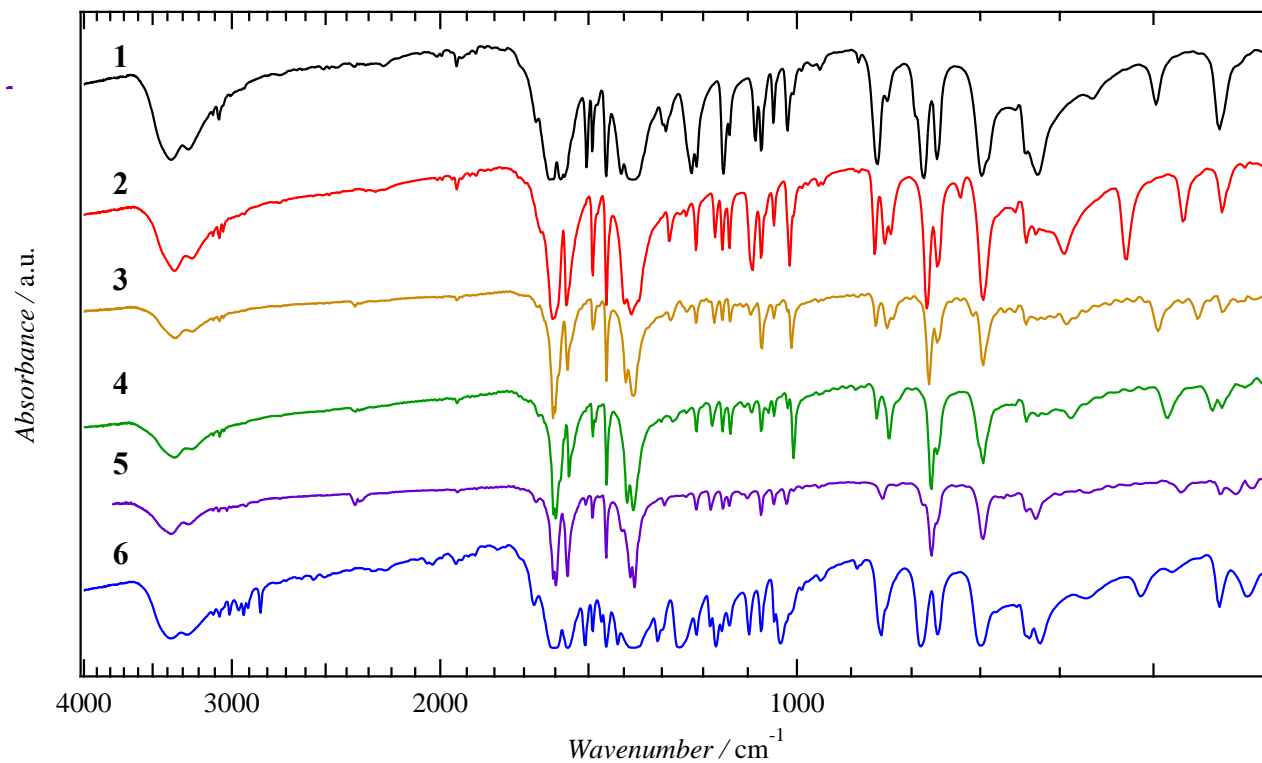


Figure S1. Infrared Spectra of **1** ~ **6**, ranged from 400 to 4000 cm⁻¹. Black, red, orange, green, purple, and blue colored lines correspond with **1**, **2**, **3**, **4**, **5** and **6** respectively.

UV-vis-NIR Diffuse Reflectance Measurement.

UV-vis-NIR diffuse reflectance spectra under ambient condition were measured for powdered sample using JASCO Model U-670 spectrometer equipped with an attachment (JASCO, ISN-723).

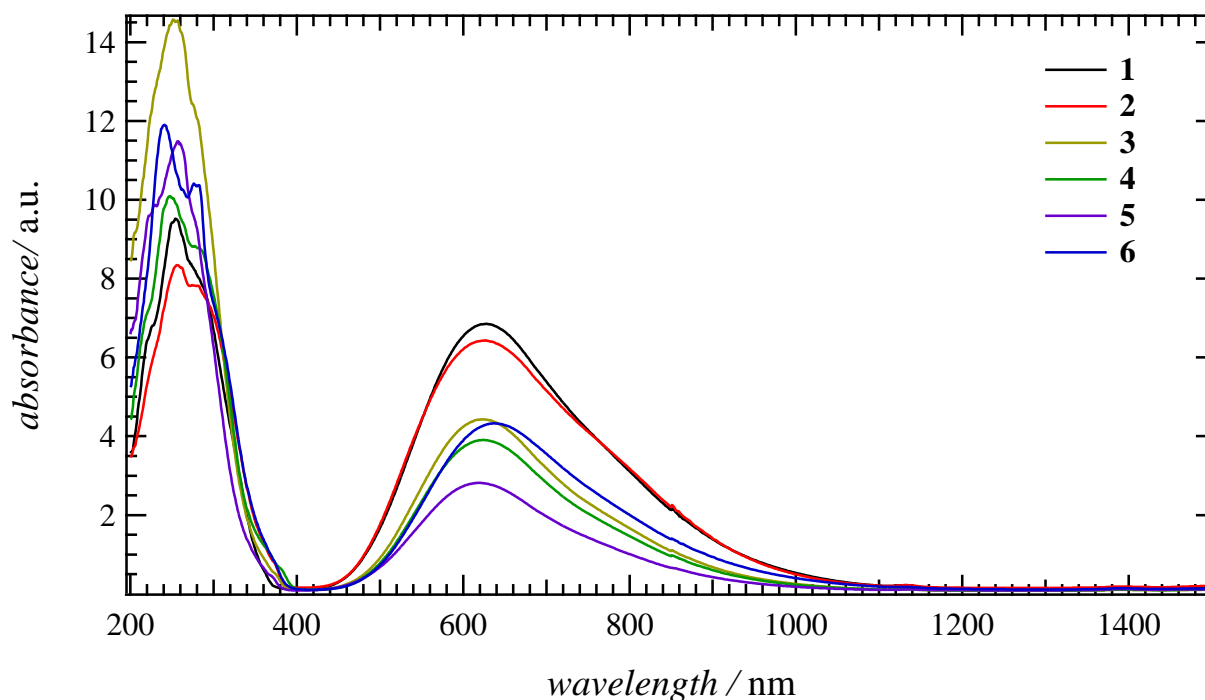


Figure S2. UV-vis-NIR diffuse reflectance spectra of **1** ~ **6**, ranged from 200 to 1500 nm. Black, red, orange, green, purple, and blue colored lines correspond with **1**, **2**, **3**, **4**, **5** and **6** respectively.

Crystal Structures

Independent structures.

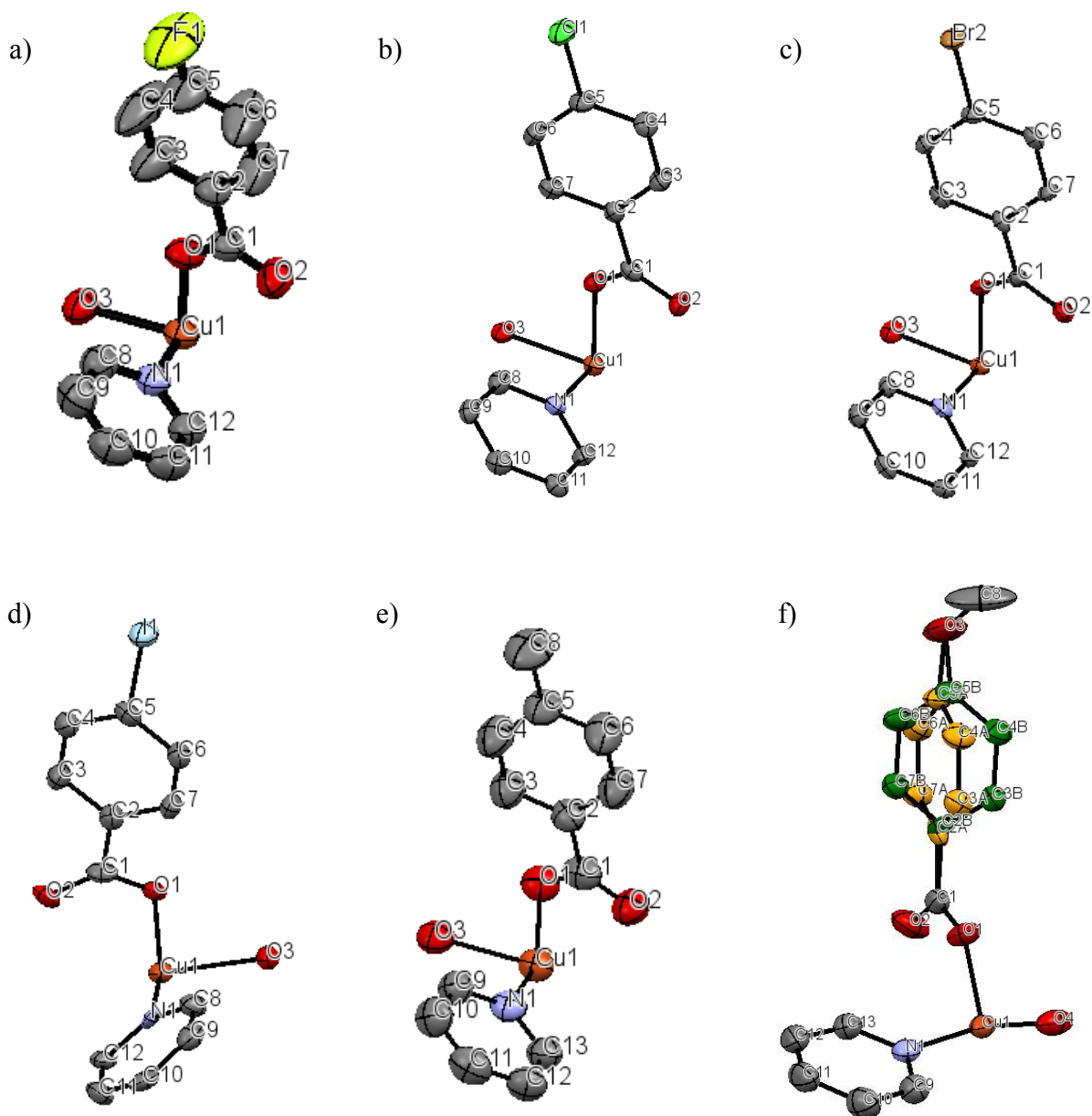


Figure S3. Crystallographic independent structures of a) **1**, b) **2**, c) **3**, d) **4**, e) **5** and f) **6** as ellipsoid model with 50% probability level. Atom labels were added near corresponding atoms. Phenyl rings colored by orange and green in crystal **6** were named **6A** and **6B**. Hydrogen atoms were omitted for clarity.

Hirshfeld Surface Analysis.

Hirshfeld surfaces were calculated by the method described in experimental section.

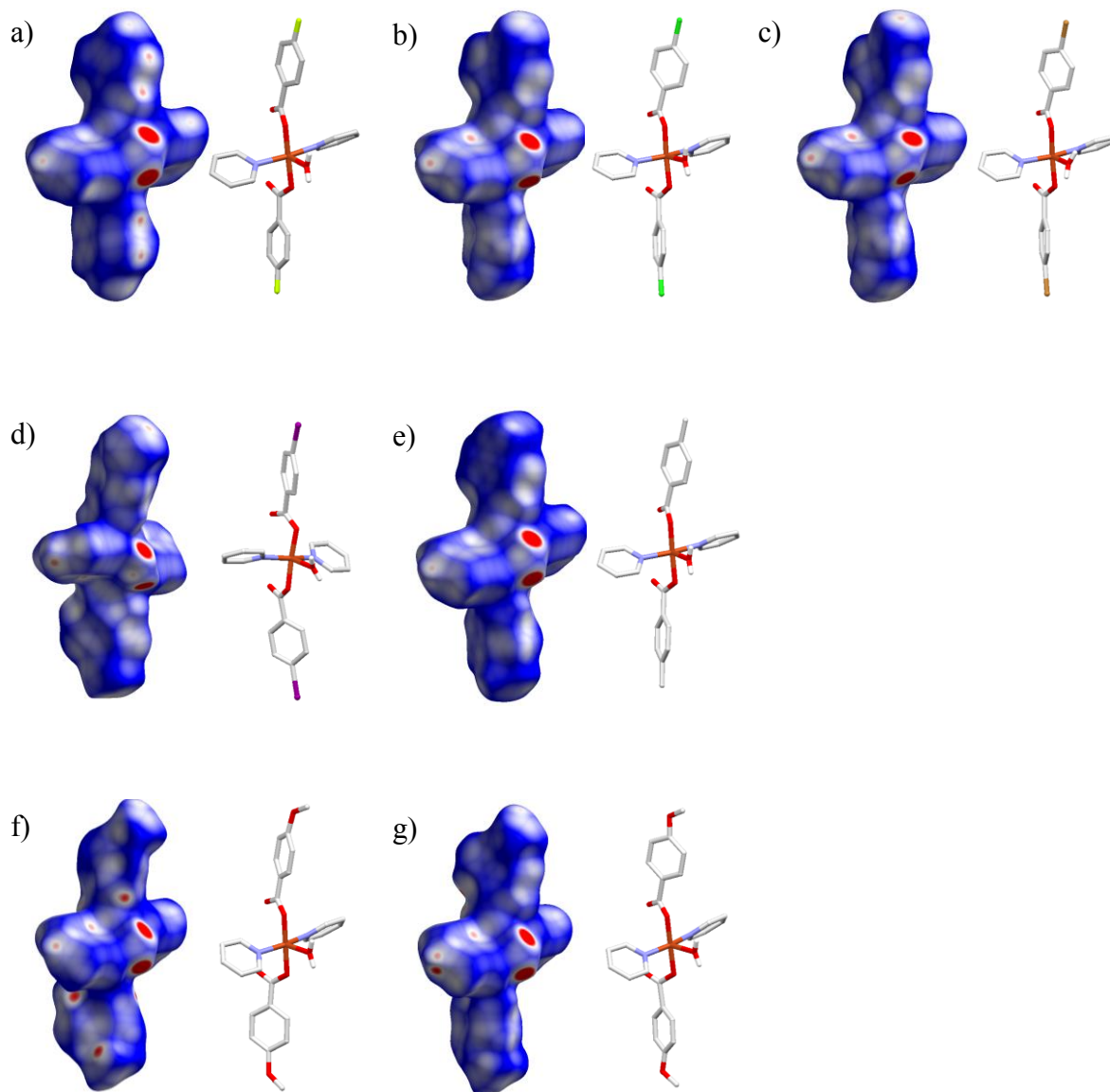


Figure S4. Visualization of intermolecular interactions using Hirshfeld surface analysis, with Hirshfeld surfaces (left figures) and molecular structures (right figures) for a) **1**, b) **2**, c) **3**, d) **4**, e) **5**, f) **6 (6A)**, and g) **6 (6B)**. The surface is defined using the parameter d_{norm} and was rescaled from -0.3 (red) to 0.8 (blue).

2D Fingerprint Plots with No Fingerprint Filtering.

2D fingerprint plots were calculated from Hirshfeld surface. Horizontal d_i and vertical d_e represent the distances from the surface to the nearest neighboring atom interior and exterior, respectively. The symbols on the upper left side of each plot indicate the numbers of crystals and disordered sites of phenyl ring in figures S3 ~ S5.

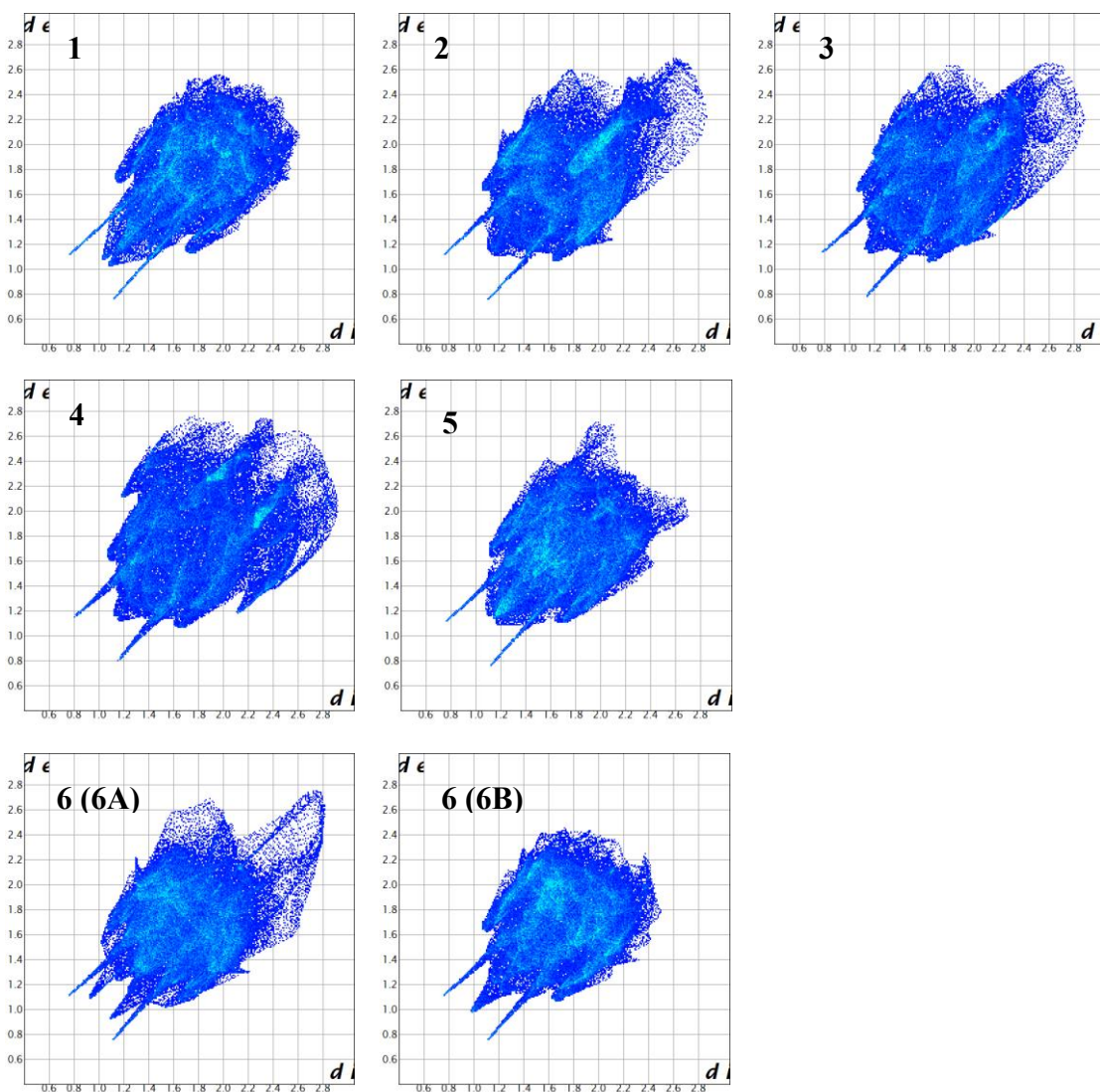


Figure S5. Fingerprint Plots of Crystal 1 ~ 6.

2D Fingerprint Plots of O...H contacts.

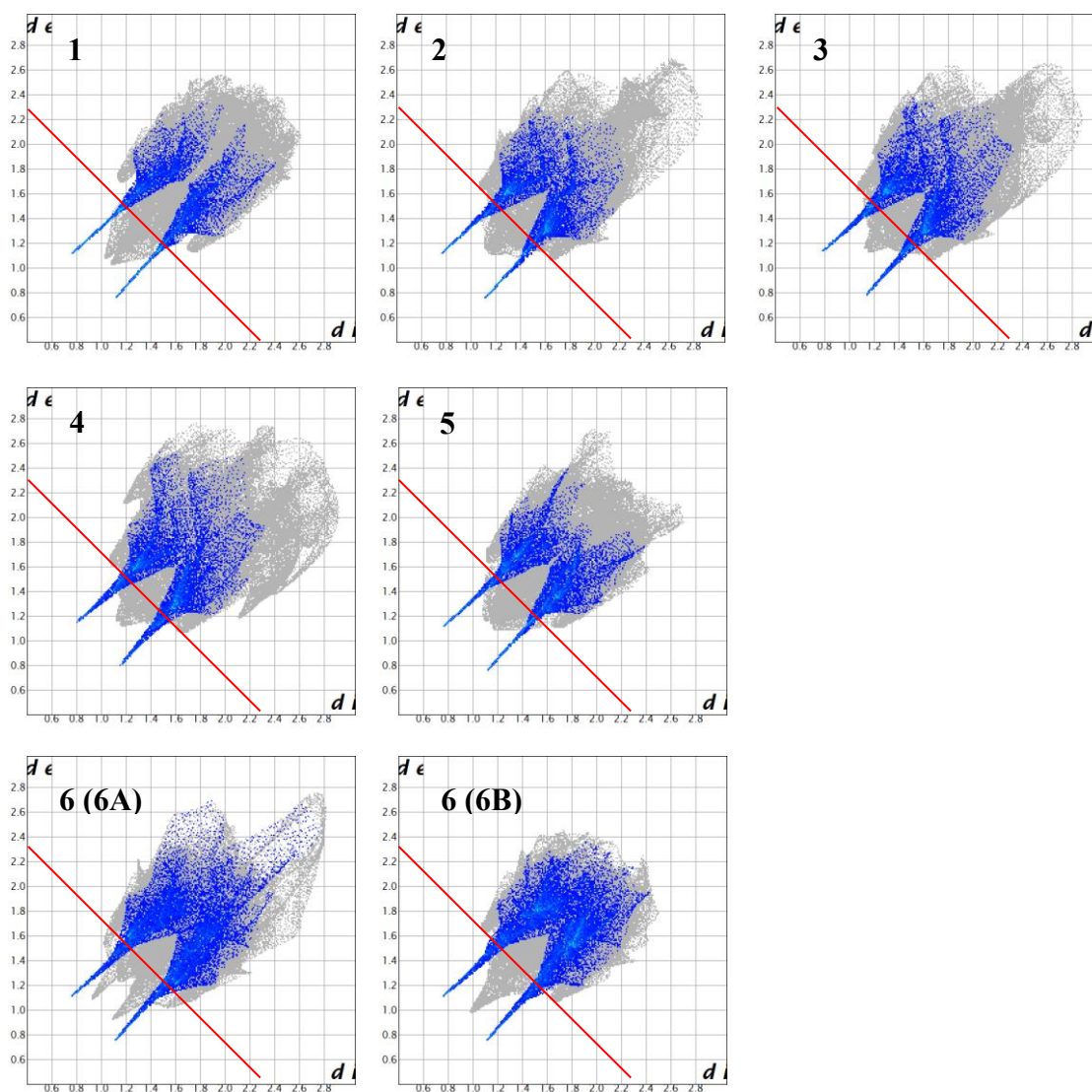


Figure S6. 2D fingerprint plots of O...H contacts (blue-colored area) along with the other kinds (gray-colored area). and a red-line was consistent with the O...H distance with the sum of the van der Waals radii of hydrogen and oxygen atoms (2.72 Å).

Each plot clearly shows that O...H contacts existed in all the crystals as hydrogen bond.

Fingerprint Plots of C···H contacts.

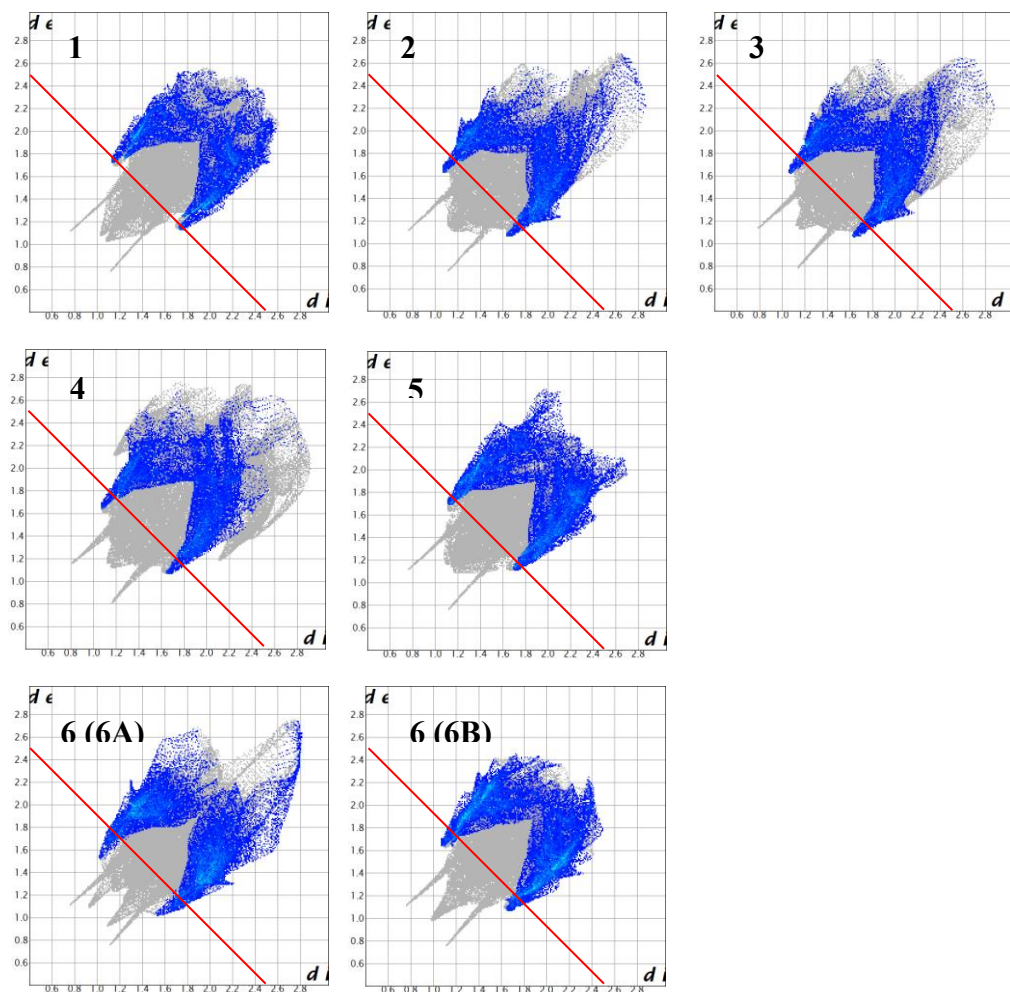


Figure S7. 2D fingerprint plots of C···H contacts (blue-colored area) along with the other kinds (gray-colored area), and a red-line was consistent with the C···H distance with the sum of the van der Waals radii of carbon and hydrogen atoms (2.9 Å).

C···H contacts shorter than the sum of van der Waals radii of carbon and hydrogen atoms were also observed in each 2D fingerprint plot of crystals **2**, **3**, **4** and **6**. On the contrary, those were not clear in crystal **1** and **5**.

Percentage Contributions of the Types of Intermolecular Interactions.

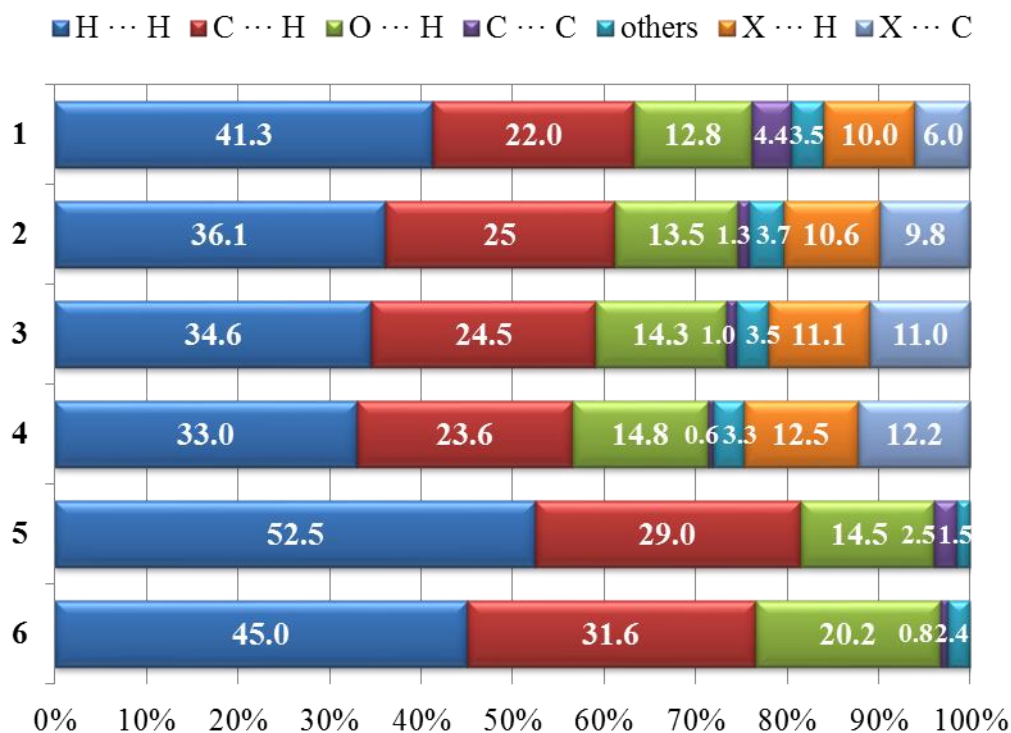


Figure S8. Histograms summarizing the types of atomic contacts between the nearest neighboring species, based on 2D fingerprint plots. The average percentages in crystals **6** were utilized due to the existence of disordered phenyl rings in *p*-MeOBA ligand.

Percentage contributions of the types of intermolecular interactions were summarized in Figure S8 as histograms. Increase in the percentage contributions related to halogen substitution in the order of **1**, **2**, **3** and **4** was compatible with increasing in the magnitudes of intermolecular interactions by each halogen substitution.

CO₂ Gas Adsorption/Desorption Property.

The CO₂ adsorption/desorption isotherms were measured for **3** and **4** with the automatic volumetric adsorption apparatus BELSORP-max (BEL Japan) at 195 K, respectively. Before the measurements, the crystals were maintained at 340 K under a pressure of less than 10⁻² Pa for 18 h in order to removed adsorbed molecules on the surface.

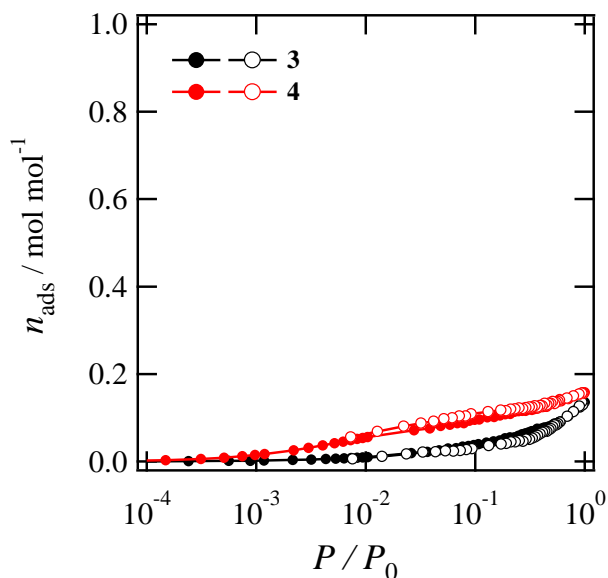


Figure S9. CO₂ adsorption/desorption isotherms at 195 K for **3** (black) and **4** (red). The adsorption and desorption processes are represented by filled and empty symbols, respectively.

One-dimensional copper complexes coordinated by pyrazine derivatives have gas adsorption/desorption properties.^{S1} The hydrogen-bonded [Cu(RBA)₂(py)₂(H₂O)] complexes also have one-dimensional structure, therefore gas adsorption property is one of the interesting research targets. However, Figure S9 showed that CO₂ adsorption/desorption properties of **3** and **4** were not observed.

REFERENCES

(S1) Takamizawa, S.; Nakata, E.; Akatsuka, T.; Miyake, R.; Kakizaki, Y.; Takeuchi, H.; Maruta, G.; Takeda, S. *J. Am. Chem. Soc.* **2010**, *132*, 3783–3792.